Structure-based virtual screening, biological assessment, and MD simulation studies of novel CNS compatible GSK-3β inhibitors as potential Alzheimer's disease therapeutics.

Sukanya Sukanya
Central University of Rajasthan
Bhanwar Singh Choudhary
Central University of Rajasthan
Pakhuri Mehta
University of Warsaw: Uniwersytet Warszawski
Slawomir Filipek
University of Warsaw: Uniwersytet Warszawski
Ruchi Malik (ruchimalik1976@curaj.ac.in)
Central University of Rajasthan https://orcid.org/0000-0002-4912-9441

Research Article

Keywords: Alzheimer's disease, Structure-based virtual screening, Glycogen synthase kinase-3β, kinase inhibitory assay, Molecular dynamic simulation.

Posted Date: February 7th, 2022

DOI: https://doi.org/10.21203/rs.3.rs-1309750/v1

Structure-based virtual screening, biological assessment, and MD simulation studies of novel CNS compatible GSK-3β inhibitors as potential Alzheimer's disease therapeutics.

Sukanya[1], Bhanwar Singh Choudhary[1], Pakhuri Mehta[2], Slawomir Filipek[2], Ruchi Malik[1]

✉ Ruchi Malik

ruchimalik1976@curaj.ac.in

Sukanya

sukanya851@gmail.com

Bhanwar S. Choudhary

bhanwarjakhar85@gmail.com

Pakhuri Mehta

pakhurimehta@gmail.com

Slawomir Filipek

sh.filipek@gmail.com

[1]Department of Pharmacy, Central University of Rajasthan, Bandarsindari, Ajmer, Rajasthan, India – 305817

[2]Faculty of Chemistry, Biological and Chemical Research Centre, University of Warsaw, ul. Pasteura 1, 02-093 Warsaw, Poland.

Abstract

Alzheimer's Disease (AD) is one of the significant diseases of the aging population and affects Central Nervous System dominantly. Blood-brain-barrier permeation is a substantial complication in developing CNS drugs, and it is considered challenging with minimal success rates. Although Glycogen synthase kinase-3β (GSK-3β) is an attractive disease-modifying target for AD, there is no single GSK-3β inhibitor in clinical trials for AD. Here we performed structure-based virtual screening on the Chembridge CNS-Set library compounds. 10 hits were identified based on interaction, binding energy, and dock score. These 10 chosen compounds showed a potential ADME profile and were then investigated for in vitro kinase inhibitory activity against GSK-3β and other AD-related kinases. Among these, the molecule 7114202 showed 48% GSK-3β inhibition while showing selectivity over other AD-related kinases. Molecular dynamic simulations of apoenzyme, co-crystallized molecule, and 7114202 validated the Lys85, Val135, Leu188, Asp200 located in the active site of enzyme plays a

significant role for GSK-3β complex formation with inhibitors, and they are responsible for activity and selectivity. The in vitro studies also revealed a potent and selective Casein Kinase 1ε (CK1ε) inhibitor 7774767 with IC_{50} 5.10 µM.

Graphical Abstract

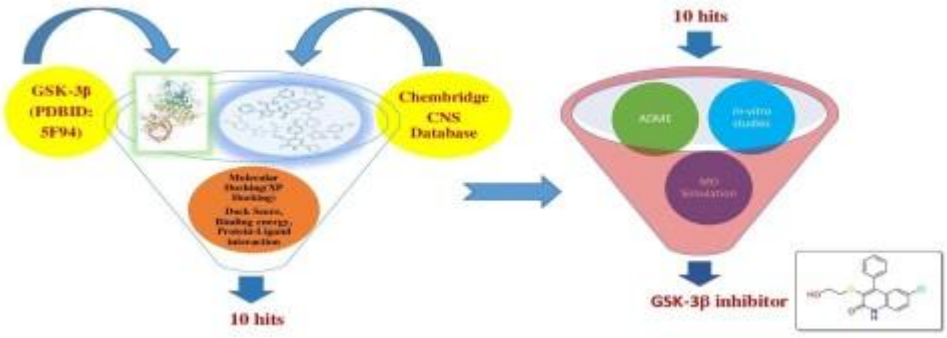

Keywords Alzheimer's disease, Structure-based virtual screening, Glycogen synthase kinase-3β, kinase inhibitory assay, Molecular dynamic simulation.

Introduction

Glycogen synthase kinase-3 (GSK-3) is a serine/threonine kinase with more than a hundred substrates, making it a needed enzyme in various cellular processes. [1] GSK-3 prevails in two isoforms (GSK-3α and GSK-3β), having 98% resemblance in their kinase domain. [2] α and β isoforms of GSK-3 are widely expressed in the body. However, their existence varies from tissue to tissue; GSK-3β isoform is principally expressed in the brain. [3] The GSK-3β enzyme has been linked with Alzheimer's Disease (AD), mood disorders [4] diabetes,[5][6] cancers, [7] cardiac hypertrophy[8], etc. AD is an irreversible, intensifying, neurodegenerative, multi-factorial disorder, one of the most typical forms of dementia. [9] Neurofibriallary tangles (NFTs) and senile plaques are the neuropathological indicators of AD. [10] NFTs are composed of phosphorylated tau proteins, and senile plaques are formed basically from amyloid-β (Aβ) peptides derived from the sequential cleavage of the amyloid precursor protein (APP) by β and γ-secretases. [10][11] The overactivity of GSK-3β leads to increased tau (microtubule-associated protein) phosphorylation which results in the destabilization of microtubules and the formation of NFTs. [12][13] overactivity of GSK-3β also results in senile plaques formation and deposition, triggering inflammatory responses, making GSK-3β an attractive target for AD. [14]. At present, there is no disease-modifying strategy available for AD treatment; the current FDA-approved drugs provide only symptomatic relief. Recent findings reveal that the focus of clinical trials in AD for the last 25 years has revolved around

AD's Aβ hypothesis. They were ineffective in retrieving cognitive function or decelerating cognitive reduction. Therefore, lowering Aβ is an unjustified strategy, and the clinical trials in AD should sharpen the attention on other AD targets comprising pathological forms of tau. [15]

Different synthetic, semi-synthetic, and natural GSK-3β inhibitors have been reported in the last two decades. These inhibitors have initially been successful to some extent in developing disease-modifying approaches for the treatment of AD. [16] Even though GSK-3β inhibitors have been reported frequently in the past few years, not a single GSK-3β inhibitor is currently in the clinical trials for AD; tideglusib, a thiazolidinedione, was withdrawn from phase II clinical trial for GSK-3β inhibition due to adverse reactions. AD is more prevalent in the aging population and affects the Central Nervous System (CNS) enormously; AD synergistically amplifies aging and its effects on the brain. The permeation of the blood-brain barrier (BBB) is a constant obstacle in CNS drug discovery. Therefore, there is a persistent requirement to explore potential GSK-3β inhibitors and prioritize drug discovery in the CNS arena. In the current study, diverse, CNS-active chemical scaffolds have been investigated and in vitro evaluated for GSK-3β inhibition to manage lead optimization adequately.

Results and Discussion

Validation of docking protocol

The docking protocol was validated by re-docking the co-crystallized ligand 2-[(cyclopropylcarbonyl)amino]-N-(4-methoxypyridin-3-yl)pyridine-4-carboxamide into the GSK-3β. The Root Mean Square Deviation (RMSD) value was found to be 0.3Å. The glide Standard Precision (SP) docking result of 80 active and 1000 decoy compounds was obtained using the pose viewer file, and the ROC (Receiver Operating Characteristic) graph was outlined (Figure 1). The ROC value after SP docking was found to be 0.99; the result represents the authenticity and stability of the docking protocol validating its adaptability for identifying structurally diverse GSK-3β inhibitors.

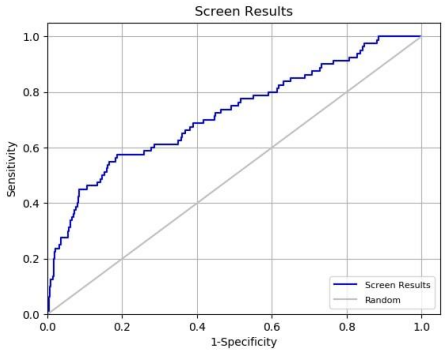

Fig. 1 The ROC graph shows docking results for 5F94 for evaluating the credibility of the docking protocol.

Structure-Based Virtual Screening

The High-throughput virtual screening (HTVS) was carried out. The hits obtained from HTVS were expeditiously docked into the protein using Glide SP; lastly, the compounds were subjected to docking employing Glide Extra Precision (XP). The best scoring docked molecules were speculated for binding affinity using Prime /MM-GBSA critical energy calculations. Each compound was docked into the GSK-3β protein, and the results were filtered based on docking score, protein ligand-interaction, and visual inspection (Table 1). All the selected compounds showed Val135 amino acid interaction. The critical amino acid interactions in the hinge region considered crucial for recognizing ATP-binding pocket are Asp133, Val135, Arg141; [17] the selected hits also showed these amino-acid interactions.

Table 1 2D interaction diagram, dock score, and MM-GBSA dG score of structure-based virtually screened hits.

S. No.	Chembridge ID	2D Interaction	Dock Score	MM-GBSA dG
1	7945239	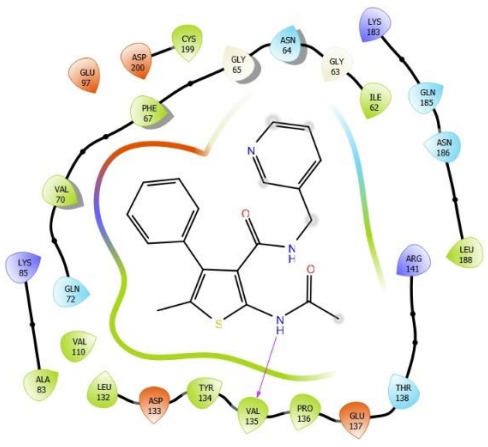	-9.968	-81.65

2	7539742	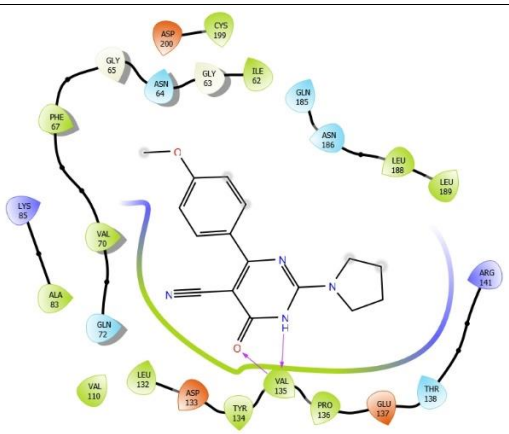	-9.621	-65.09
3	6329758	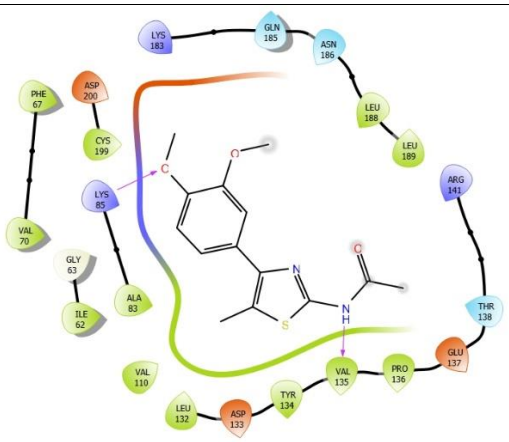	-9.577	-78.53
4	6644998	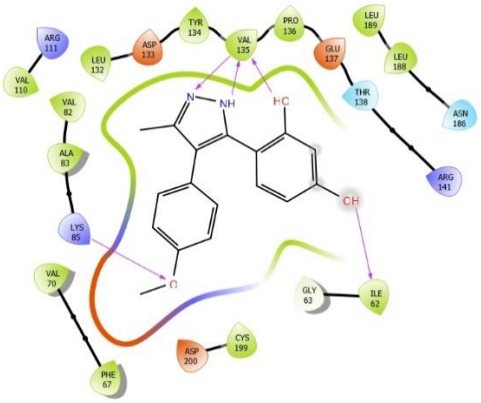	-9.494	-83.01
5	7520529	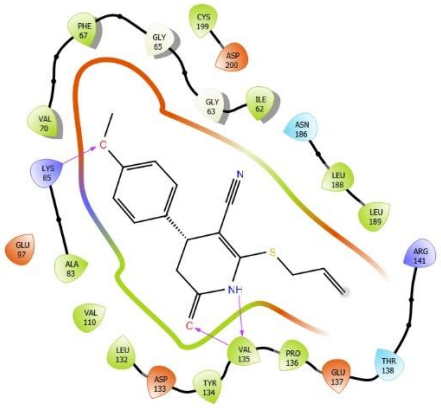	-9.182	-82.51

6	7763406	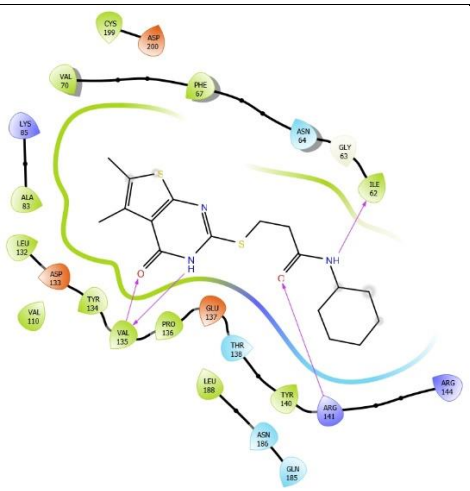	-8.324	-92.12
7	5473348	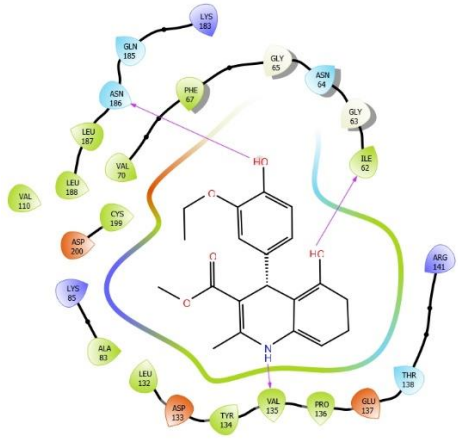	-8.806	-82.86
8	7114202	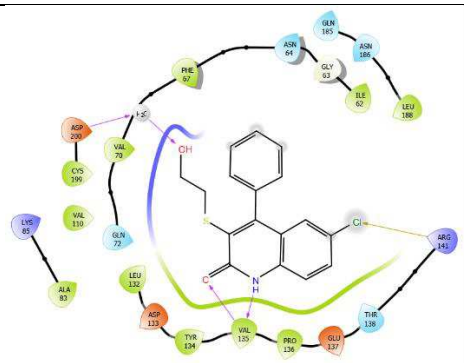	-8.292	-79.33
9	5807166	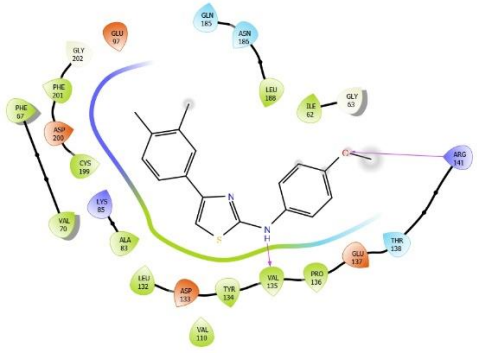	-8.424	-79.15

10	7774767	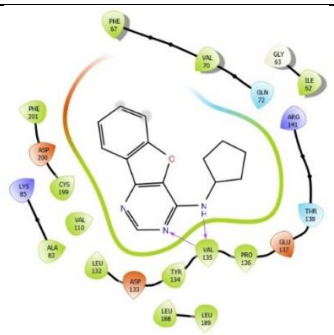	-9.058	-77.04

ADME Analysis

The 10 selected hits were subjected to ADME analysis using the *QikProp* module of Schrodinger. The qualifying preferred ranges for the CNS oral drugs were used to predict the pharmacokinetic properties of these compounds (Table 2).

Table 2 ADME properties prediction of best scoring hits using *QikProp*.

S. No.	Chembridge ID	% HOA	SASA	Donor HB	Acceptor HB	log O/W	log S	Log BB	PCaco	PMDCK	Log Khsa	HOA	Rule of 5	Rule of 3	CNS	Polrz
Range →		61 to 100	348 to 798	0 to 3	1 to 8.3	-0.16 to 6.0	-6.5 to -0.42	-1.2 to 1.2	0 to 3629	0 to 5899	-1 to 1.04	2 to 3	0 to 1	0 to 1	-2 to 2	14 to 49
1	7945239	100	603.741	1	5.5	3.825	-4.826	-0.374	1418.96	1252.62	0.411	3	0	0	0	38.239
2	7539742	86.198	590.065	1	6.25	2.051	-5.295	-1.061	436.241	201.808	-0.04	3	0	0	-2	32.882
3	6329758	100	568.067	1	5.5	2.81	-4.404	-0.165	2269.06	2140.31	0.026	3	0	0	0	31.169
4	6644998	89.169	543.841	3	3.25	2.651	-4.163	-0.959	406.694	187.075	0.241	3	0	0	-1	31.666
5	7520529	95.119	577.079	1	4.75	2.961	-5.393	-0.845	692.544	471.364	0.176	3	0	0	-1	31.825
6	7763406	90.972	626.265	2	6	2.682	-4.03	-0.616	501.035	1066.9	-0.014	3	0	0	0	36.258
7	5473348	100	624.097	2	3.75	3.888	-5.313	-0.914	654.231	312.735	0.678	3	0	1	-1	36.947
8	7114202	96.429	554.183	2	4.7	3.118	-4.241	-0.6	728.165	1120.92	0.119	3	0	0	0	32.108
9	5807166	100	599.216	1	2.75	5.013	-5.935	0.331	6575.3	7055.49	0.771	3	1	1	1	36.012
10	7774767	100	509.28	1	3	3.26	-4.159	-0.071	2904.99	1566.59	0.274	3	0	0	0	29.068

The Lipinski parameters like Partition coefficient, hydrogen bond donor, hydrogen bond acceptor, molecular weight were all in the preferred range for the top 10 selected hits. The other ADME properties like percentage human oral absorption, predicted o/w partition coefficient (log Po/w), predicted blood-brain partition coefficient (log BB), apparent Caco -2 permeability (P Caco), predicted binding to human serum albumin (Log Khsa), predicted polarizability in Å (Polrz), predicted apparent MDCK cell permeability (PMDCK) were all in permissible limit for CNS oral drugs. Solvent accessible surface area (SASA) and qualitative CNS activity parameters were in the qualifying range for all the selected 10 molecules. None of the compounds were found to violate Lipinski's rule of 5 and Jorgensen's rule of 3, suggesting the selected hits showed favorable ADME properties as CNS drug candidates. Afterward, the selected 10 virtual hits were subjected to in vitro assay against GSK-3β and a short panel of disease-related kinases.

Kinase Assay

The selected hits showed promising pharmacokinetic parameters and were subjected for kinase profiling at 10 µM concentration against other disease-related kinases along with GSK-3β. The in vitro inhibitory activity of these selected hits against Cyclin-Dependent Kinase 2 (CDK2), Cyclin-Dependent Kinase 5 (CDK5), Glycogen Synthase Kinase 3β (GSK-3β), CDC-2 Like Kinase1 (CLK1), Casein kinase I isoform epsilon (CK1ε), and Dual-specificity tyrosine phosphorylation-regulated kinase 1A (DYRK1A) was determined. Two compounds showed GSK-3β inhibition, one of the compounds 7114202, showed selective inhibition of the GSK-3β enzyme. Selective inhibition of DYRK1A and CK1ε was also demonstrated by compounds 5807166 and 7774767, respectively (Table 3). Compound 7114202 showed nearly 50% GSK-3β inhibition with selectivity over other AD-related kinases. Compound 6644998 inhibited both GSK-3β/DYRK1A equally (36%) and CK1ε (32%), showing multi-enzyme inhibition. This study also led to the identification of CNS compatible compound 7774767 as a CK1ε inhibitor (60%) with a high degree of selectivity over DYRK1A, GSK-3β, and other disease-related kinases and compound 5807116 as DYRK1A inhibitor (40%) with selectivity over other kinases. Based on inhibitory activity, the compounds 7774767, 7114202, and 5807166 were selected for IC_{50} determination against CK1ε, GSK-3β, and DYRK1A, respectively (Figure 2). Compounds 7114202 and 5807166 showed IC_{50} > 100 µM, whereas compound 7774767 showed 5.10 µM IC_{50} for CK1ε. (Table 4) CK1ε is an important circadian regulator, and this enzyme is overexpressed in AD.[18] The inhibition of CK1ε has been reported to improve cognitive-affective behavior and amyloid burden[19]; hence indicating CK1ε kinase is a therapeutic target for AD. Synthetic molecules similar to 7774767 have been reported as dual inhibitors of CK1ε and DYRK1A. [20] 7774767 has O substituted in place of previously reported S/NH substitution. A cyclopentane ring is attached to NH in place of NH_2, which may be responsible for making the compound 7774767 a highly selective inhibitor of CK1ε over DYRK1A and other kinases in the panel.

Table 3: Percentage activity of kinases in the presence of 10 µM concentration of 10 selected compounds.

S. No.	Compound ID	CDK2	CDK5	GSK-3β	CLK1	CK1ε	DYRK1A
1.	**5807166**	≥100	87	96	96	75	**58**
2.	5473348	97	≥100	95	≥100	88	70
3.	6329758	≥100	≥100	98	≥100	73	78
4.	**6644998**	92	≥100	**64**	74	**68**	**64**
5.	**7114202**	≥100	≥100	**52**	89	82	82
6.	7520529	≥100	≥100	≥100	≥100	≥100	≥100
7.	7539742	≥100	≥100	≥100	≥100	≥100	≥100
8.	7763406	≥100	≥100	79	≥100	95	≥100

9.	**7774767**	≥100	85	91	86	**40**	90
10.	7945239	92	≥100	98	≥100	98	78

*ATP concentration used in kinase assay 10µmol/L (values are given as means, n=2). ≥100 indicates that the compound cannot inhibit the enzymatic activity at the tested concentration.

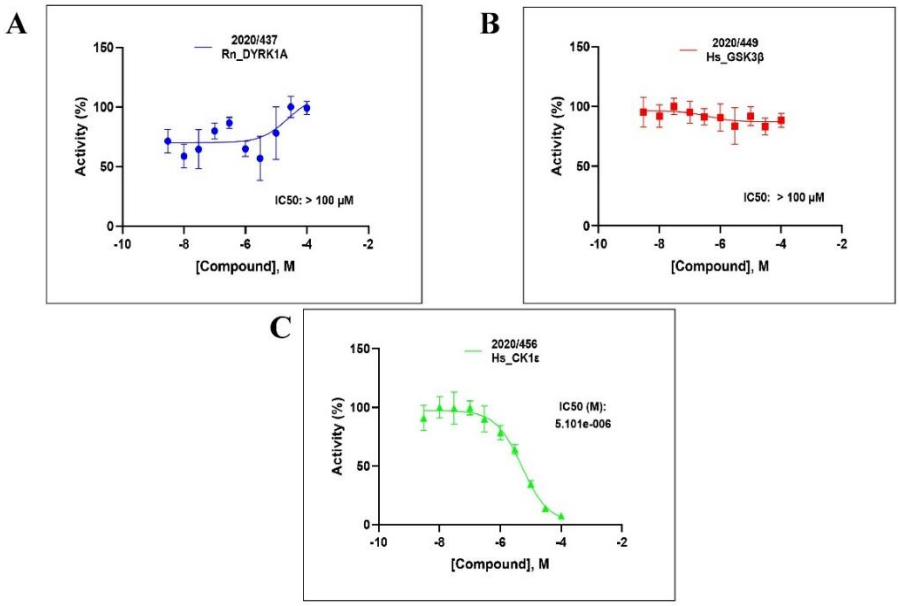

Fig. 2 Dose-response curve of **A** compound 5807166 against DYRK1A. **B** compound 7114202 against GSK-3β. **C** compound 7774767 against CK1ε, respectively. (Error bars in 2C where they are not visible are smaller))

Table 4 IC_{50} (in µM) of compounds 5807166, 7114202, and 7774767.

S. No.	Compound ID	DYRK1A	GSK-3β	CK1ε
1.	5807166	>100	NT	NT
2.	7114202	NT	>100	NT
3.	7774767	NT	NT	**5.10**

*NT: not tested for specific kinase. Data are expressed as means of duplicate measurements.

Molecular Dynamics Simulation Study

The compound 7114202 showed maximum inhibition of GSK-3β and was subsequently picked out for Molecular Dynamic (MD) simulation studies. Here, we reported two MD simulation systems comprising one apo system and one GSK-3β protein (5F94) with the compound 7114202 (receptor-ligand complex). The simulation was carried out for 50ns for both systems to predict protein stability, several protein-ligand interactions, functional features, and binding mode.

The RMSD was calculated for both the MD simulation systems. Under the influence of the force field, the RMSD value of any system from 0-3Å is acceptable for a stable system having a normal behavior in a specific condition. The RMSD of both systems showed an initial bounce

at 0ns, representing the little accustoming of the protein system in the solvent condition. The RMSD value of the apo system and the protein-ligand complex was 1.5 and 1.75, respectively. RMSD value of the co-crystalized ligand previously reported is around 1.75. The Root Mean Square Fluctuation (RMSF) value annotates the active site analysis of GSK-3β and unveils the conformational changes in the protein chain. The RMSF value of amino acid residues in the binding pocket of the apo system and the protein-ligand complex was observed fluctuating lower than 2.5Å (Figure 3).

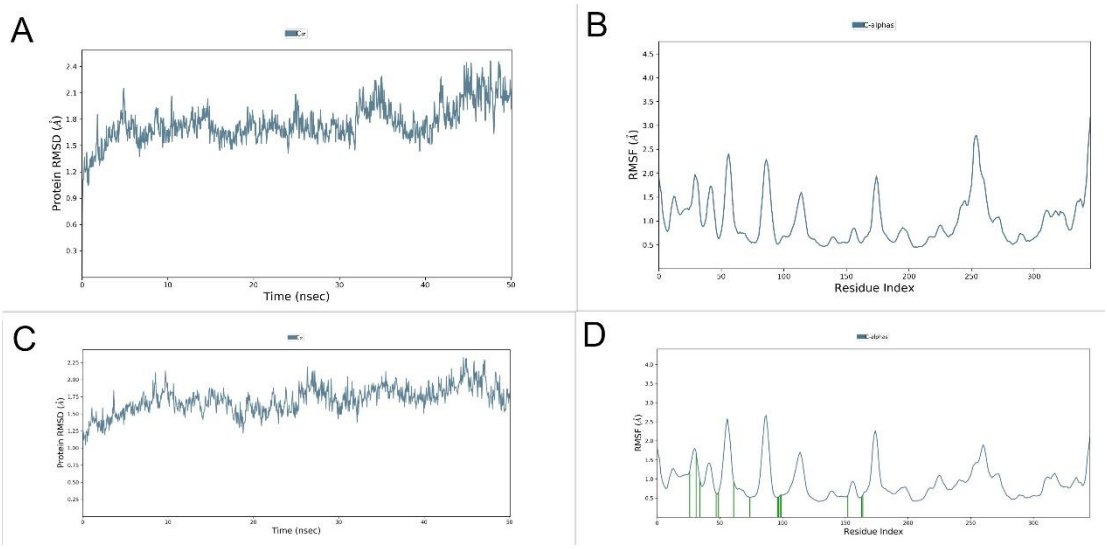

Fig. 3 A RMSD of GSK-3β protein. **B** RMSF of GSK-3β protein. **C** RMSD of GSK-3β-7114202. **D** RMSF of GSK-3β-7114202

The corresponding protein-ligand interaction within the binding pocket of GSK-3β protein and the compound 7114202 were observed. The critical interactions included (i) the hydrogen bond established by quinolin-2(1H)-one ring system of the screened hit (7114202) with amino acid residue Val135 backbone of the hinge region. Hydrogen bond interaction of the ligand with Val135 amino acid residue of protein has been reported in various active GSK-3β inhibitors (16). This interacting hinge region of GSK-3β has been described as the region responsible for molecular recognition, and this interaction is responsible for enhanced affinity. [17][16] (ii) hydrogen-bonded protein-ligand interactions mediated by a water molecule in the polar region by residue Lys 85 and Asp200 with the terminal OH of the aliphatic side chain of the molecule (7114202). These interactions are essential for selectivity against other kinases. [21] Lys 85 and Asp 200 are also essential for ATP recognition as Lys85 interacts with the phosphate group of ATP.[22] (iii) hydrophobic interactions were observed with the ligand by amino acid residue Val70 and Leu188 (Figure 4). In our previous work, we have reported the protein-ligand interactions of co-crystallized molecules. The significant interactions include hydrogen bond

of the ligand with Val135 residue, water-bridge mediated hydrogen bonds by Lys85 and Asp200, and hydrophobic interactions by Phe67, Ala83, and Leu188. [23] The molecule (7114202) showed similar protein-ligand interactions as the co-crystallized molecule, substantiating the MD simulation study carried out on it.

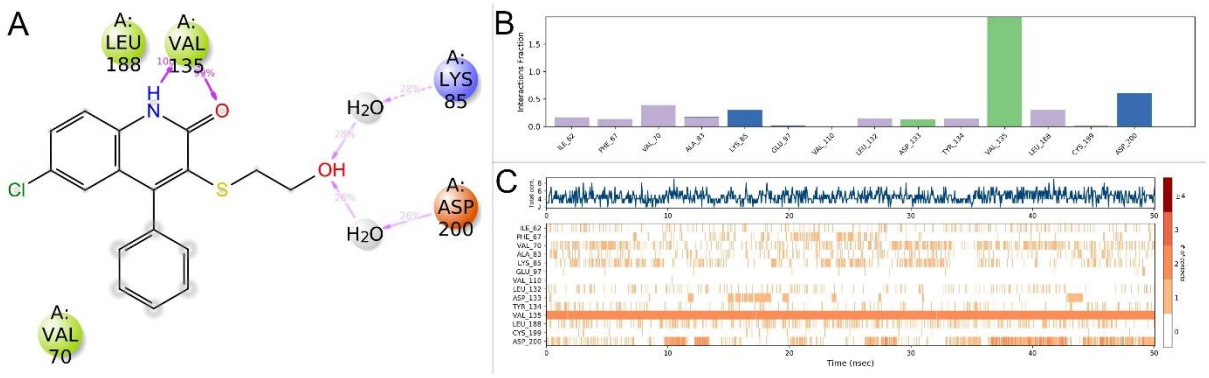

Fig. 4 A Ligand protein interaction observed during the simulation study of the 7114202-GSK-3β complex; **B** Histogram depicting the amino acid interactions of the 7114202-GSK-3β complex; **C** Timeline representing protein-ligand interaction observed during 50 ns simulation with GSK-3β and 7114202

Conclusion

In the quest to find the disease-modifying AD treatment, the CNS-compatible small molecules database was investigated as GSK-3β inhibitors. We performed structure-based virtual screening on the Chembridge CNS-Set library compounds to identify potential GSK-3β inhibitors. The selected compounds were investigated over a small panel of kinases, including GSK-3β. While most of the compounds were inactive, compound 7114202 showed 48% GSK-3β inhibition with selectivity over other kinases; compound 6644998 showed equal inhibition of GSK-3β/DYRK1A and inhibited CK1ε 32%, depicting multi-target inhibition. We also found that compound 7774767 inhibited CK1ε up to 60%, and compound 5807166 inhibited DYRK1A up to 42% with high selectivity over other kinases in the panel. Based on enzyme inhibition shown by these compounds, three compounds were further selected for IC_{50} calculations. Interestingly compound 7774767 showed IC_{50} 5.10μM against CK1ε. Furthermore, MD simulation studies revealed various protein-ligand interactions in the ATP binding pocket of the enzyme. The critical interactions in the hinge region- Val135, water-bridge mediated interaction-Lys85, and Asp200, hydrophobic interaction-Ala83, and Leu188 gave insight into the microscopic superfast events taking place within seconds in the enzyme. The protein-ligand interactions were familiar with the co-crystallized molecule and reported in

previous literature, justifying the structure-based virtual screening and MD simulation studies. The interaction of Lys85 with the terminal hydroxyl group of 7114202 advocates for compound selectivity over other kinases, and the interaction in hinge regions like Val135, Leu188 favors the inhibitory activity of 7114202. The compound 7114202 is a quinolone derivative. This class has rarely been explored as GSK-3β inhibitors; this study reveals the quinolone class as a potential framework for designing selective GSK-3β inhibitors and testifies our findings using the computational approach. SAR analysis of identified hits may be helpful in developing selective and potential GSK-3β inhibitors in the future. Also, CK1ε is fascinating and less explored kinases for AD; compound 7774767 may serve as potential leads that can structurally be optimized to highly selective CK1ε inhibitors. This study demonstrates that these CNS compatible molecules may serve as booming lead compounds for designing and developing selective kinase inhibitors (single, dual or multi-target approaches) and paves the way for promising disease-modifying AD treatment.

Materials and Methods

Protein preparation and receptor grid generation

The crystal structure of GSK3β bound to 2-[(cyclopropylcarbonyl)amino]-N-(4-methoxypyridin-3-yl)pyridine-4-carboxamide (PDB ID: 5F94) was retrieved from Protein Data Bank. [24] The protein structure was processed by using protein preparation wizard*, Epik* version 3.4 (Maestro, version 10.4);[25] The grid around an active site of protein was generated, and the coordinates of the co-crystallize ligand around the center point of the active site of the receptor were defined using the receptor grid generation panel of Glide version 2020-1.

Compound library selection and ligand preparation

Using the Chembridge CNS-Set library of 61041 compounds were downloaded from Chembridge portal. Ligand preparation was carried out using Ligprep (2.5 application) version 2020-1 (from Schrodinger software); the energetical minimization of structures stereoisomers generation at neutral pH was performed using ionizer and OPLS 2005 forcefield subprograms. [26][27]

Structure-based virtual screening

Docking protocol was validated by docking the co-crystallized molecule and determining its RMSD value by superimposing co-crystallized and docked molecule (2-[(cyclopropylcarbonyl)amino]-N-(4-methoxypyridin-3-yl)pyridine-4-carboxamide). The

protein validation was performed by enrichment calculation. 80 reported GSK-3β inhibitors from the literature and 1000 decoy compound set were merged, and a structural evaluation database was assembled containing 1080 compounds. This database was docked against the GSK-3β receptor using the SP docking method of Glide software. Subsequently, the ROC curve and AUC (area under the curve) were obtained by enrichment calculator.

The docking protocol encompasses the standard protocols provided by Schrodinger for the virtual screening of large databases. HTVS, SP, and XP docking were performed and outlined for the Chembridge CNS-Set library of 61041 compounds. 10% of the compounds obtained from HTVS were subjected to SP, and a further 10% of the compounds were carried forward from SP to XP. Prime/MM-GBSA obtained binding energy calculations on the complexes obtained post XP docking. Finally, the top 10 scoring compounds were selected based on their structural features, docking score, fundamental interactions reported for GSK-3β in literature, binding energy, and nature of interaction with GSK-3β active site amino acid residues.

Estimation of ADMET properties

ADMET analysis, an indispensable tool in drug discovery, predicts initial hits' pharmacokinetics. The ADMET properties of the selected hits obtained after structure-based virtual screening were assessed using the software QikProp 4.6 version of Schrodinger (Maestro, version 10.4). The obtained hits were analyzed for computed physicochemical and Pharmacokinetic properties using the qualifying and preferred ranges parameters for CNS oral drugs. [28]

ADP-Glo Kinase assay

It is a highly sensitive, unique, and consistent assay for determining kinases and ATPases activity utilizing a large variety of substrates. The high sensitivity of this assay is helpful in monitoring enzyme activities even if the quantity of enzyme is meager. This assay is composed of two steps: the first step is the addition of ADP-Glo reagent for terminating the reaction and exhausting any leftover ATP. The second step is the addition of another reagent for converting this reaction into light using a luciferase reaction. The light generated is proportional to ADP present, resembling the kinase or ATPase activity. [29] ADP-Glo^{TM} bioluminescent kinase assay kit (Promega, Madison, WI) was used to perform protein kinase assay per the manufacturer's guidelines.[30] Precisely, kinase inhibitory activities of 10 selected compounds were assayed in a 384-well plate against GSK-3β and a short panel of Disease-related kinases. The reactions were executed in a concluding volume of 6µl for 30 min at 30°C in suitable

kinase buffer with peptide as substrate in the presence of 10µM ATP. Subsequently, to cease the reaction, 6µl of ADP-Glo TM Reagent was added. Eventually, after incubating for 50 min at room temperature (RT), 12µl of Kinase Detection Reagent was added for 1 hour at RT. The Envision (PerkinElmer, Waltham, MA) microplate luminometer measured the transmitted signal and denoted it in the Relative Light Unit (RLU).

Buffer: 10mM $MgCl_2$, 1mM EGTA, 1 mM DTT, 25 mM Tris-HCl pH 7.5, 50 µg/ml heparin.

Kinases: *Hs*CDK2/CyclinA, (Cyclin-Dependent kinase 2, kindly provided by Dr. A. Echalier-Glazer, Leicester, UK) was assayed in buffer A with 0.8 µg/µl of histone H1 as substrate.

*Hs*CDK5/p25 (human, recombinant, expressed in bacteria) was assayed with 0.8 µg/µl of histone H1 as substrate.

HsGSK-3β (human, recombinant, expressed by baculovirus in Sf9 insect cells) were assayed with 0.010 µg/µl of GS-1 peptide, a GSK-3β-selective substrate (YRRAAVPPSPSLSRHSSPHQSpEDEEE).

MmCLK1 (from Mus musculus, recombinant, expressed in bacteria) was assayed with 0.027µg/µl of the peptide: GRSRSRSRSRSR as substrate.

SscCK1ε (casein kinase 1ε, porcine brain, native, affinity-purified) was assayed with 0.022 µg/µl of the following peptide: RRKHAAIGSpAYSITA ("Sp" stands for phosphorylated serine) as CK1-specific substrate.

RnDYRK1A-kd (Rattus norvegicus, amino acids 1 to 499 including the kinase domain, recombinant, expressed in bacteria, DNA vector kindly provided by Dr. W. Becker, Aachen, Germany) was assayed with 0.033 µg/µl of peptide: KKISGRLSPIMTEQ as substrate. [31]

To determine the half-maximal inhibitory concentration (IC_{50}), these assays were performed in the absence or presence of increasing doses of the tested compounds in duplicate. Kinase activities were expressed in percentage of maximal activity, i.e., measured in the absence of inhibitor. The peptide substrates were obtained from Proteogenix (Schiltigheim, France). [32][33]

Molecular Dynamics Simulations

MD Simulations help understand microscopic events like ligand binding and important macromolecular movements connected to it that take place in less than a second. [34] Full-atom MD simulations were performed for the GSK-3β protein and the best screened hit using *Desmond* version 2014.2 (Maestro, version 10.4). The MD simulation process comprises three steps: the system builder, minimization, and molecular dynamics. Simple point charge (SPC) solvent model and Phosphatidylcholine (POPC) membrane with an orthorhombic boundary

box were used for building the model. The system was further neutralized using 0.15 M of Na^+ and Cl^-.

The system was put through energy minimization to rule out any stearic conflicts. The simulation studies of 50ns were performed post equilibration of a complex system finished with the constant-temperature constant-pressure (NPT) ensemble at 300K temperature and pressure of 1 bar for a protein-ligand complex of 7114202-GSK-3β and apoprotein. The RMSD of protein, Protein RMSF, and Ligand RMSF were calculated after the MD simulations using md.out.cms file.

Acknowledgments

The authors are grateful to the Central University of Rajasthan for providing a licensed Schrodinger molecular modeling software facility and KISSf, Station Biologique, Roscoff, France, for support in the screening of our compounds against kinases. Dr. Ruchi Malik is thankful to the Department of Science and Technology, India for financial support (Grant No.: INT/FRG/DAAD/P-10/2018). Sukanya is grateful to the Council of Scientific and Industrial Research, India for CSIR Senior Research Fellowship (Grant No.: 09/1131(0026)/19-EMR-I).

Conflict of Interest

The authors report there are no competing interests to declare.

References

1. Sutherland C. What are the bona fide GSK3 substrates? International Journal of Alzheimer's Disease. Int J Alzheimers Dis. 2011;2011:505607. doi:10.4061/2011/505607.

2. Eldar-Finkelman H. Glycogen synthase kinase 3: An emerging therapeutic target. Trends Mol Med. 2002;8(3):126–32. doi:10.1016/s1471-4914(01)02266-3.

3. Soutar MPM, Kim WY, Williamson R, Peggie M, Hastie CJ, McLauchlan H et al. Evidence that glycogen synthase kinase-3 isoforms have distinct substrate preference in the brain. J Neurochem. 2010;115(4):974–83. doi:10.1111/j.1471-4159.2010.06988.x.

4. Hsiung SC, Adlersberg M, Arango V, Mann JJ, Tamir H, Liu KP. Attenuated 5-HT1A receptor signaling in brains of suicide victims: Involvement of adenylyl cyclase, phosphatidylinositol 3-kinase, Akt and mitogen-activated protein kinase. J Neurochem. 2003;87(1):182–94. doi:10.1046/j.1471-4159.2003.01987.x.

5. Gum RJ, Gaede LL, Koterski SL, Heindel M, Clampit JE, Zinker BA et al. Reduction of protein tyrosine phosphatase 1B increases insulin-dependent signaling in ob/ob mice. Diabetes. 2003;52(1):21–8. doi:10.2337/diabetes.52.1.21.

6. Ring DB, Johnson KW, Henriksen EJ, Nuss JM, Goff D, Kinnick TR et al. Selective glycogen synthase kinase 3 inhibitors potentiate insulin activation of glucose transport and utilization in vitro and in vivo. Diabetes. 2003;52(3):588–95. doi:10.2337/diabetes.52.3.588.

7. Inoki K, Ouyang H, Zhu T, Lindvall C, Wang Y, Zhang X et al. TSC2 Integrates Wnt and Energy Signals via a Coordinated Phosphorylation by AMPK and GSK3 to Regulate Cell Growth. Cell. 2006;126(5):955–68. doi:10.1016/j.cell.2006.06.055.

8. Morisco C, Seta K, Hardt SE, Lee Y, Vatner SF, Sadoshima J. Glycogen Synthase Kinase 3β Regulates GATA4 in Cardiac Myocytes. J Biol Chem. 2001;276(30):28586–97. doi: 10.1074/jbc.M103166200.

9. Querfurth HW, Laferla FM. Alzheimer's Disease. N Engl J Med. 2018;362(4);329–44. doi:10.1056/NEJMra0909142.

10. St George-Hyslop PH. Piecing together Alzheimer's. Sci Am. 2000;283(6):76–83. doi:10.1038/scientificamerican1200-76.

11. Bloom GS. Amyloid-β and tau: The trigger and bullet in Alzheimer disease pathogenesis. JAMA Neurol. 2014;71(4):505–8. doi:10.1001/jamaneurol.2013.5847.

12. Hanger DP, Hughes K, Woodgett JR, Brion J-P, Anderton BH. Glycogen synthase kinase-3 induces Alzheimer's disease-like phosphorylation of tau: generation of paired helical filament epitopes and neuronal localisation of the kinase. Neurosci Lett. 1992;147:58-62. doi:10.1016/0304-3940(92)90774-2.

13. Mazanetz MP, Fischer PM. Untangling tau hyperphosphorylation in drug design for neurodegenerative diseases. Nat Rev Drug Discov. 2007;6:464–79. doi:10.1038/nrd2111.

14. Hooper C, Killick R, Lovestone S. The GSK3 hypothesis of Alzheimer's disease. J Neurochem. 2008;104(6):1433–9. doi:10.1111/j.1471-4159.2007.05194.x.

15. Oxford AE, Stewart ES, Rohn TT. Clinical Trials in Alzheimer's Disease: A Hurdle in the Path of Remedy. Int J Alzheimers Dis. 2020;2020:5380346. doi:10.1155/2020/5380346.

16. Khan I, Tantray MA, Alam MS, Hamid H. Natural and synthetic bioactive inhibitors of glycogen synthase kinase. Eur J Med Chem. 2017;125:464-77. doi:10.1016/j.ejmech.2016.09.058.

17. Arfeen M, Bhagat S, Patel R, Prasad S, Roy I, Chakraborti AK et al. Design, synthesis and biological evaluation of 5-benzylidene-2-iminothiazolidin-4-ones as selective GSK-3β inhibitors. Eur J Med Chem. 2016;121:727–36. doi:10.1016/j.ejmech.2016.04.075.

18. Perez DI, Gil C, Martinez A. Protein kinases CK1 and CK2 as new targets for neurodegenerative diseases. Med Res Rev. 2011;31(6):924–54. doi:10.1002/med.20207.

19. Sundaram S, Nagaraj S, Mahoney H, Portugues A, Li W, Millsaps K et al. Inhibition of casein kinase 1δ/εimproves cognitive-affective behavior and reduces amyloid load in the APP-PS1 mouse model of Alzheimer's disease. Sci Rep. 2019;9:13743. doi:10.1038/s41598-019-50197-x.

20. Loidreau Y, Dubouilh-Benard C, Nourrisson M-R, Loaëc N, Meijer L, Besson T et al. Exploring Kinase Inhibition Properties of 9H-pyrimido[5,4-b]- and [4,5-b]indol-4-amine Derivatives. Pharmaceuticals. 2020;13(5):89. doi:10.3390/ph13050089.

21. Chun K, Park JS, Lee HC, Kim YH, Ye IH, Kim KJ et al. Synthesis and evaluation of 8-amino-[1,2,4]triazolo[4,3-a]pyridin-3(2H)-one derivatives as glycogen synthase kinase-3 (GSK-3) inhibitors. Bioorganic Med Chem Lett. 2013;23:3983–7. doi:10.1016/j.bmcl.2013.03.119.

22. Maqbool M, Mobashir M, Hoda N. Pivotal role of glycogen synthase kinase-3: A therapeutic target for Alzheimer's disease. Eur J Med Chem. 2016;107:63–81. doi: 10.1016/j.ejmech.2015.10.018.

23. Choudhary BS, Sukanya, Mehta P, Bach S, Ruchaud S, Robert T et al. Discovery of thiazolidin-4-one analogue as selective GSK-3β inhibitor through structure based virtual screening. Bioorganic Med Chem Lett. 2021;52:128375. doi:10.1016/j.bmcl.2021.128375.

24. Luo G, Chen L, Burton CR, Xiao H, Sivaprakasam P, Krause CM et al. Discovery of Isonicotinamides as Highly Selective, Brain Penetrable, and Orally Active Glycogen Synthase Kinase-3 Inhibitors. J Med Chem. 2016;59(3):1041–51. doi:10.1021/acs.jmedchem.5b01550.

25. Madhavi Sastry G, Adzhigirey M, Day T, Annabhimoju R, Sherman W. Protein and ligand preparation: Parameters, protocols, and influence on virtual screening enrichments. J Comput Aided Mol Des. 2013;27(3):221–34. doi:10.1007/s10822-013-9644-8.

26. Jorgensen WL, Maxwell DS, Tirado-Rives J. Development and testing of the OPLS all-atom force field on conformational energetics and properties of organic liquids. J Am Chem Soc. 1996;118(45):11225–36. doi:10.1021/ja9621760.

27. Shivakumar D, Williams J, Wu Y, Damm W, Shelley J, Sherman W. Prediction of absolute solvation free energies using molecular dynamics free energy perturbation and the OPLS force field. J Chem Theory Comput. 2010;6(5):1509–19. doi:10.1021/ct900587b.

28. Ghose AK, Herbertz T, Hudkins RL, Dorsey BD, Mallamo JP. Knowledge-based, central nervous system (CNS) lead selection and lead optimization for CNS drug discovery. ACS Chem Neurosci. 2012;3:50–68. doi:10.1021/cn200100h.

29. Zegzouti H, Zdanovskaia M, Hsiao K, Goueli SA. ADP-Glo: A bioluminescent and homogeneous ADP monitoring assay for Kinases. Assay Drug Dev Technol. 2009;7:560–72. doi:10.1089/adt.2009.0222.

30. Corporation P. ADP-Glo Kinase Assay. 2011. https://www.promega.in/products/cell-signaling/kinase-assays-and-kinase-biology/adp-glo-kinase-assay/?catNum=V6930.

31. Qhobosheane MA, Legoabe LJ, Josselin B, Bach S, Ruchaud S, Petzer JP et al. Synthesis and evaluation of 7-azaindole derivatives bearing benzocycloalkanone motifs as protein kinase inhibitors. Bioorg Med Chem. 2020;28(11):115468. doi:10.1016/j.bmc.2020.115468.

32. Lechner C, Flaßhoff M, Falke H, Preu L, Loaëc N, Meijer L et al. [b]-Annulated Halogen-Substituted Indoles as Potential DYRK1A Inhibitors. Molecules. 2019;24(22):4090. doi:10.3390/molecules24224090.

33. Brikci-Nigassa NM, Bentabed-Ababsa G, Erb W, Chevallier F, Picot L, Vitek L et al. 2-Aminophenones, a common precursor to N-aryl isatins and acridines endowed with bioactivities. Tetrahedron. 2018;74:1785–801. doi:10.1016/j.tet.2018.02.038.

34. Choi SB, Yap BK, Choong YS, Wahab H. Molecular dynamics simulations in drug discovery. Encyclopedia of Bioinformatics and Computational Biology. 2019. doi:10.1016/B978-0-12-809633-8.20154-4.